Steven Adler-Golden, Nevzat Guler and Timothy Perkins, “Atmospheric correction of commercial thermal infrared hyperspectral imagery using FLAASH-IR," Proc. SPIE 10644, Algorithms and Technologies for Multispectral, Hyperspectral, and Ultraspectral Imagery XXIV (8 May 2018).

DOI: https://doi.org/10.1117/12.2305146

See next page for full paper.

Atmospheric correction of commercial thermal infrared hyperspectral imagery using FLAASH-IR

Steven Adler-Golden*, Nevzat Guler and Timothy Perkins
Spectral Sciences, Inc., Burlington, MA 01803

ABSTRACT

Within the last few years, several commercial long-wave infrared (LWIR) hyperspectral imaging (HSI) systems have been developed for remote sensing of the ground from aircraft. While much less expensive and more practical to operate than sensors such as SEBASS and MAKO, which have been developed primarily for research and Government use, the commercial systems have poorer signal-to-noise and/or spectral resolution. We investigate the utility of three commercial systems—the Telops Hyper-Cam, SPECIM AisaOWL, and ITRES TASI-600—for quantitative retrieval of surface temperature and emissivity spectra. Atmospheric retrieval, correction and temperature-emissivity separation are performed on example data from these sensors using FLAASH-IR, a first-principles algorithm that incorporates radiation transport calculations and atmosphere models from MODTRAN. The results from the commercial sensors are noisy compared with SEBASS but otherwise appear to be reasonable. Applying a noise suppression algorithm to the radiance data yields better temperature retrievals and much cleaner emissivity spectra, with minimal loss of information, and should benefit scene classification applications.

Keywords: LWIR, hyperspectral, noise suppression, atmospheric correction, Hyper-Cam, AisaOWL, TASI-600

1. INTRODUCTION

Hyperspectral imaging (HSI) technology provides a wealth of information for remotely identifying and characterizing surface materials and objects based on their spectral signatures. Long-wave infrared (LWIR) HSI sensors yield both surface emissivity spectra and temperatures if the atmospheric effects are removed—a process called atmospheric correction or compensation—and the surface emission is factored into emissivity and Planck function components—a process called temperature-emissivity separation (TES). Relevant atmospheric conditions relating to temperature, water vapor, and ozone are generally unknown, and therefore must be retrieved from the image as part of this processing.

Atmospheric compensation is formally an underdetermined problem: both the emissivity spectrum and temperature for a given pixel are presumably unknown, so that, even with a precisely known atmosphere, the number of unknowns exceeds the number of spectral radiance values. Atmospheric correction and TES solutions have been developed using a variety of constraints on the spectrum and atmospheric representation in combination with a variety of mathematical methods. In this paper we show results from the FLAASH-IR (Fast Line-of-sight Atmospheric Analysis of Spectral Hypercubes – InfraRed) algorithm[1] with airborne imagery from several commercial HSI sensors.

We have previously reported on FLAASH-IR results from an airborne Telops Inc. Hyper-Cam LW[2]. Here we show results from Hyper-Cam data of better quality, as well as results from the ITRES TASI-600 and SPECIM AisaOWL sensors. These commercial sensors all have much higher noise levels than the state-of-the art sensors such as the Aerospace Corp.'s SEBASS[3] and MAK0[4]. However, the noise problem can be substantially mitigated by pre-processing the radiance data with a noise suppression algorithm. We include FLAASH-IR results from data processed with a new method that suppresses noise with little or no degradation of the true spectral emissivity features.

*adlergolden@spectral.com; phone 1 781 273-4770; fax 1 781-270-1161; spectral.com

2. FLAASH-IR METHOD

We briefly review the FLAASH-IR atmospheric correction and TES method. The LWIR spectral radiance measured by a sensor viewing objects on the ground can be written as

$$L_{obs}(\lambda) = B(T, \lambda)\varepsilon(\lambda)\tau(\lambda) + [1 - \varepsilon(\lambda)]L^{\downarrow}(\lambda) + L^{\uparrow}(\lambda) \quad (1)$$

where λ is wavelength, $\varepsilon(\lambda)$ is the composition- and temperature-averaged spectral emissivity of the surface pixel, $\tau(\lambda)$ is the total (diffuse plus direct) transmittance between the surface and the sensor, $B(T, \lambda)$ is the surface Planck blackbody function at temperature T, $L^{\downarrow}(\lambda)$ is the transmitted incident illumination, and $L^{\uparrow}(\lambda)$ is the atmospheric path radiance. T is effectively an emissivity-weighted average within each pixel. Eq. (1) is rigorous for Lambertian surfaces.

The FLAASH-IR algorithm solves the radiance equation (1) for horizontal surfaces and scene-average atmospheric spectra. Trial atmospheres are modeled using MODTRAN6®[5] by starting from a layered approximation to a standard MODTRAN model atmosphere and forming a 3-D look-up table (LUT) by modifying the temperature, water vapor and ozone profiles. The retrieved atmospheric $\tau(\lambda)$, $L^{\downarrow}(\lambda)$ and $L^{\uparrow}(\lambda)$ spectra are interpolates from this 3-D LUT that minimize a total in-band squared radiance error σ^2 summed over a selected set of *i* diverse pixels:

$$\sigma^2 = \sum_i \sum_\lambda [L_{iobs}(\lambda) - L_i(\underline{\varepsilon(\lambda)})]^2 \quad (2)$$

The $L_i(\underline{\varepsilon(\lambda)})$ are predicted pixel radiances based on emissivities that are spectrally smoothed with a running average over adjacent wavelengths, typically five. That is, the quantity to be minimized is a measure of the difference between the actual pixel radiances and those predicted from smoothed emissivities corresponding to a trial atmosphere and trial pixel temperatures. The σ^2 minimization is carried out using golden section searches for the pixel surface temperatures embedded within a 3-D Nelder-Mead simplex search for the atmosphere. Once the atmosphere is retrieved, the temperature and spectral emissivity or reflectance (i.e., 1-emissivity) is derived for each pixel in the scene using the golden section search.

3. FLAASH-IR CONFIGURATION FOR DIFFERENT SENSORS

FLAASH-IR has a few setup parameters that require adjustment for each sensor.

Wavelength Range for Retrievals. The atmosphere retrieval should be performed over the wavelength range where the signal-to-noise is high, the wavelength calibration is accurate, and the atmosphere is not too opaque. Typically, this range extends from around 8.1 μm to the longest clean wavelength band, which depends on the focal plane material. However, a higher starting wavelength may be preferred for sensors that have significant variation in the wavelength calibration across the image. With these sensors, it can be beneficial to restrict the wavelength range for TES to the ozone band region of ~9.0-10.2 μm, as this band is more robust to wavelength mismatch than the water vapor lines that dominate elsewhere. Otherwise, the same wavelength range may be used for the atmosphere retrieval and the TES.

Instrument Resolution Function. FLAASH-IR offers a choice of Gaussian, triangular and sinc resolution functions. The sinc function is appropriate for unapodized Fourier transform infrared (FTIR) spectra. Gaussians of appropriate full width at half maximum (FWHM) satisfactorily approximate most other resolution functions, include FTIR spectra with commonly used apodizations.

Spectral Recalibration Option. FLAASH-IR offers the option to automatically refine the spectral calibration by deriving and applying a wavelength shift and stretch and a scaling of the FWHMs. This step involves minimization of the Eq. (2) radiance error within loops over the calibration parameters, and typically improves the results with grating spectrometers. The spectral recalibration step is generally unnecessary with FTIR spectrometers.

Normalized Emissivity Method (NEM) Option. FLAASH-IR offers the option of performing the TES with a normalized emissivity method (NEM), in which the maximum emissivity is set to a fixed value, taken as 0.98. The NEM may give better results than the smooth emissivity (σ^2 minimization) method when atmospheric features are weak—for example, with a dry atmosphere or when spectral resolution is limited—and when the materials of interest are natural.

FLAASH-IR currently exists in two versions. An IDL-language version has been developed for use within the ENVI (Harris Corp.) software package and has a graphical user interface. A C++-language version has a text file interface, making it suitable for batch operation, and it directly supports Telops Hypercam file formats.

4. NOISE SUPPRESSION ALGORITHM

Background thermal noise in LWIR HSI can be minimized through aggressive cooling of the sensor and selecting state-of-the-art focal plane arrays, but these measures are very expensive. Consequently, there has been considerable interest in noise suppression through data post-processing. Among the most successful methods for HSI are those based on the maximum noise fraction (MNF) transform[6,7]. A linear operator describing the sensor noise variance or covariance is estimated from either the data itself or a sensor specification. The data are then multiplied by the inverse square root of the operator, which "whitens" the noise, and the result is subjected to a principal component (PC) transformation. The PC transformation projects the spectra onto the eigenvectors of the spectral covariance matrix of the noise-whitened data. The noise whitening and PC transformation can be combined in a single linear operation comprising the MNF transform. The MNF eigenimages (i.e., projection coefficient images) corresponding to very small eigenvalues (comparable to the noise variance) are dominated by noise. "De-noised" data are recovered by suppressing coefficients that are deemed to be noise-dominated and then applying the inverse MNF transform.

Various strategies have been developed for the MNF coefficient suppression step[8]. The challenge is to suppress noise while minimally disturbing the valid small-eigenvalue coefficients that belong to rare spectra. We have recently developed a new method based on Bayesian signal estimation, described in a patent application[9]. In brief, the "true," noise-free MNF coefficients are estimated from the observed ones, y, by multiplying by a shrinkage function, given by

$$S(y) = 1 / [r \exp(-y^2) + 1] \qquad (3)$$

where r is a positive eigenimage-dependent constant. The shrinkage function suppresses small values of y. Eq. (3) derives from a simplified representation of the noise-free coefficients' probability distribution function (PDF) as the sum of a delta function and a flat distribution. The former describes pixels whose true coefficients in the eigenimage are negligibly small, while the latter describes pixels whose true coefficients exceed the noise level. The r value reflects the proportions of these two classes of pixels in the eigenimage PDF and is estimated from statistics of the y values.

An example of de-noising overhead Hyper-Cam LW radiance data is shown in Figure 1. In contrast to the original spectra, which have noise at the several microflick RMS level, the fine structure in the de-noised spectra is almost entirely real and of atmospheric origin. There appears to be somewhat less noise suppression in the reflective spectra, which are uncommon, compared to the spectra of more abundant materials, consistent with their sparser MNF representations (i.e., higher proportion of noise-dominated coefficients).

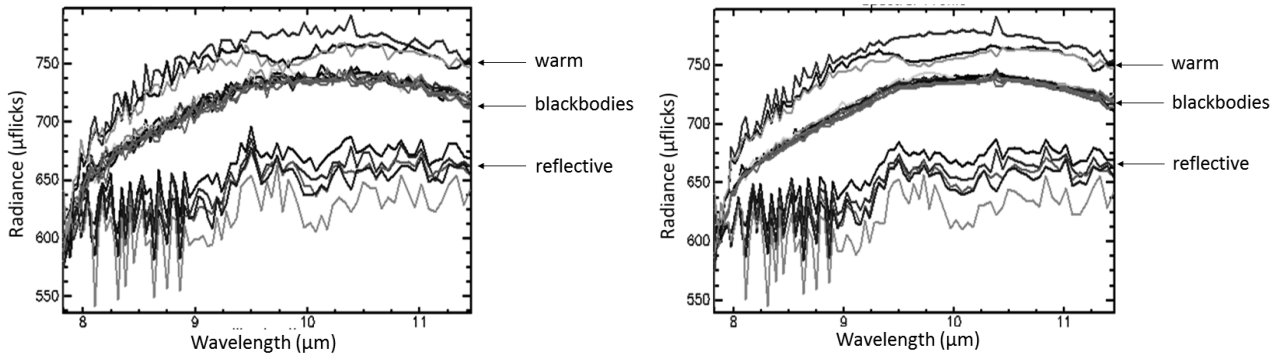

Figure 1. Hyper-Cam LW radiance spectra of a rock quarry before (left) and after (right) de-noising.

5. DATA AND RESULTS

Hyper-Cam LW. The Hyper-Cam LW, manufactured by Telops Inc. (Quebec City, Canada), is a portable imaging FTIR spectrometer for the 8-12 µm spectral range. The detector is a Stirling-cooled 320x256 PV-MCT focal plane array detector with useful response out to around 11.5 µm. The pixel IFOV is 0.35 mrad, and spectral resolution is user selectable from 0.25 to 150 cm-1. The system has been integrated into an aircraft platform for nadir-viewing measurements, with acquisition times of typically ~1 s. Overlapping images are acquired and assembled into georectified mosaics.

A FLAASH-IR analysis of early Hyper-Cam LW aircraft data appears in a previous paper[2]. Improvements in the stability of the system have resulted in reduction of artifacts, and, when combined with the de-noising algorithm, yield emissivity spectra of good quality. Example FLAASH-IR outputs are shown in Figures 2 and 3 for a mosaic image acquired in April, 2013 of farmland south of Quebec City. The image, which includes metal-roofed buildings, shows substantial spectral diversity. Spectral resolution, at 6 cm^{-1} (0.06 µm at 10 µm), is ample for material classification, as seen most clearly with the de-noised data. The de-noising has a stabilizing effect on the TES, as can be seen in the improved agreement in absolute emissivity between two different pixels of what is likely the same material (black and violet curves).

Figure 2. False color detail images of reflectance (red = 8.5 µm, green = 9.5 µm, blue = 10.5 µm), from FLAASH-IR processing of a Hyper-Cam LW mosaic of farmland near Quebec City. At left, without de-noising; at right, with de-noising.

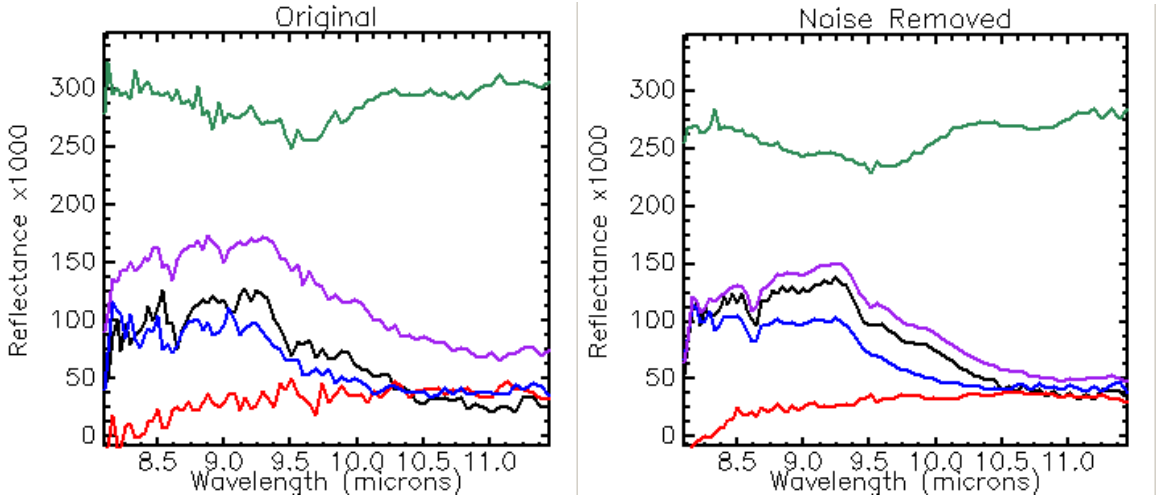

Figure 3. FLAASH-IR reflectance spectra from the Figure 2 scene, without (left) and with (right) de-noising.

AisaOWL. The AisaOWL[10], manufactured by Spectral Imaging Limited (SPECIM), Oulu, Finland, is a pushbroom grating spectrometer with around 100 bands covering 7.7-12.3 μm with 0.10 μm resolution. The detector is a Stirling-cooled MCT focal plane array. The pixel IFOV is selectable as either 1.1 or 1.5 mrad. Overlapping images are acquired and are assembled into georectified mosaics.

Figure 4 shows a false-color FLAASH-IR emissivity image (left) and selected spectra (right) from a small portion of a data strip taken at South Cornelly, UK. The image, which shows a stone quarry, was taken from an altitude of 0.6 km; our radiance de-noising algorithm was applied. Several different minerals in the quarry are identifiable by color in the emissivity image, and their spectra are distinct. The results are considerably poorer without the de-noising step. The noise level is somewhat higher with the AisaOWL than with the HyperCam, but this is not surprising, considering that its useful spectral response extends to longer wavelengths.

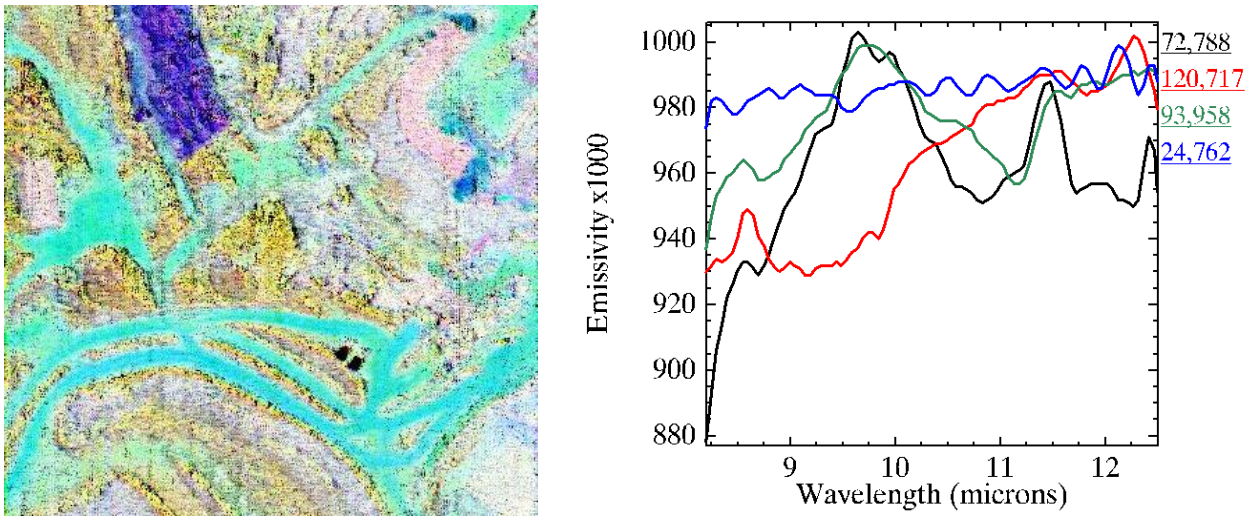

Figure 4. FLAASH-IR emissivities from an AisaOWL image of the South Cornelly, UK, stone quarry; denoising was applied. At left, a portion of the image in false color (RGB = 8.5, 10.0, 11.5 μm). At right, representative spectra.

TASI-600. The TASI-600[11], manufactured by ITRES Research Limited, Calgary, Canada, is an airborne pushbroom prism spectrometer with 32 bands covering 8-11.5 μm. We estimate the spectral resolution as slightly wider than the band spacing of 0.11 μm. The cryogenically cooled MCT detector provides 600 cross-track pixels; the pixel IFOV is 1.2 mrad. Overlapping images are acquired and assembled into georectified mosaics.

Figure 5 shows FLAASH-IR emissivity spectra from an image of Cuprite, NV taken from 1.6 km above the ground. Mineral assignments are based on comparisons with higher resolution spectra retrieved by FLAASH-IR from SEBASS[12] and with spectra from the John Hopkins University minerals library degraded to the TASI-600 spectral resolution, shown at right. The level of spectral resolution and the desert conditions of this scene make it a good candidate for the NEM, results from which are shown at center without de-noising. For this scene and these natural materials, the absolute emissivities from the NEM are more accurate than those from the smooth-emissivity method, which produces some emissivities that slightly exceed 1, as well as others that appear to be too low, not shown in Figure 5. These results are consistent with an analysis by McDowell and Kruse[13] of MAKO imagery for similar desert terrain, in which FLAASH-IR atmosphere retrievals were combined with the NEM for TES. The best results for the current scene use FLAASH-IR with the NEM and de-noising; Figure 6 shows a 710 x 570 m portion of the emissivity image in false color. The blue, magenta and yellow areas respectively correlate with the presence of quartz, alunite and calcite.

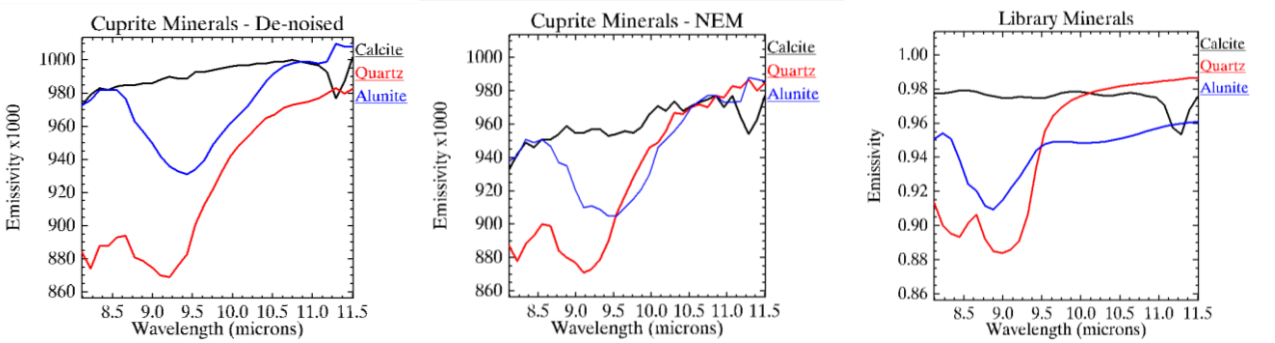

Figure 5. Comparison of emissivity spectra from a TASI-600 image of Cuprite, NV with mineral spectra from the JHU library.

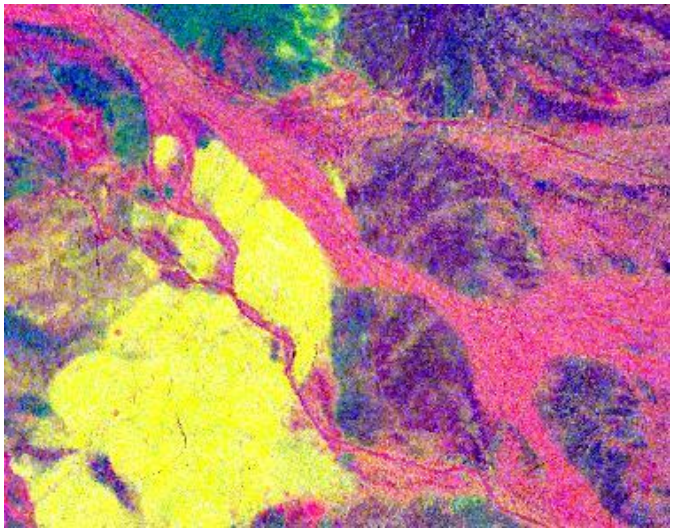

Figure 6. A portion of the Cuprite de-noised NEM emissivity image in false color (RGB = 8.2, 10.0, 11.5 μm).

6. SUMMARY AND CONCLUSIONS

Processing LWIR HSI to reflectance or emissivity via atmospheric correction and TES affords the ability to classify and identify solid materials with minimal interference from the atmosphere. This paper shows results from processing airborne data from three different commercial LWIR HSI sensors using FLAASH-IR and an optional noise suppression algorithm. There were no difficulties in applying FLAASH-IR to these sensors, and, as far as can be determined without having ground truth, the retrieved reflectances or emissivities are very reasonable.

The three sensors studied differ in noise level, spectral and spatial resolution, and spectral coverage, and this preliminary work does not attempt to rank their performance. However, we conclude that the data from all of the sensors are of sufficient quality for many applications in scene material classification, including mineral identification, especially when the data are processed with a noise suppression technique. It remains to be seen whether the data have enough signal-to-noise for more stressing applications such as detecting rare materials or small, low-concentration gas plumes. Since noise suppression relies on spectral aggregation, either directly or indirectly through decomposition into basis components, it may not improve the detection of rare spectra.

7. ACKNOWLEDGEMENTS

This work was supported by Spectral Sciences, Inc. (SSI) internal research and development. We thank Martin Chamberland (Telops), Jason Howse (ITRES) and Timo Hyvarinen (SPECIM) for providing SSI with the hyperspectral imagery.

8. REFERENCES

[1] Adler-Golden, S.M., Conforti, P., Gagnon, M., Tremblay, P. and Chamberland, M., "Long-wave infrared surface reflectance spectra retrieved from Telops Hyper-Cam imagery," Proc. SPIE Algorithms and Technologies for Multispectral, Hyperspectral, and Ultraspectral Imagery XX, 90880, doi:10.1117/12.2050446 (2014a).

[2] Adler-Golden, S.M., Conforti, P., Gagnon, M., Tremblay, P. and Chamberland, M., "Remote sensing of surface emissivity with the Telops Hyper-Cam," Proc. 6th WHISPERS Conference, Lausanne, 24-27 June (2014b).

[3] Hackwell, J.A., D.W. Warren, R.P. Bongiovi, S.J. Hansel, T.L. Hayhurst, M.G. Sivjee, and J.W. Skinner, "LWIR/MWIR imaging hyperspectral sensor for airborne and ground-based remote sensing," SPIE Proceedings, Imaging Spectrometry, Vol. 2819, pp. 102-107 (1996).

[4] Warren, D.W.; Boucher, R.H.; Gutierrez, D.J.; Keim, E.R.; Sivjee, M.G., "MAKO: A high-performance, airborne imaging spectrometer for the long-wave infrared," Proc. SPIE, 7812 (2010).

[5] Berk, A. and F. Hawes, "Validation of MODTRAN®6 and its line-by-line algorithm," J. Quant. Spectrosc. Radiat. Transfer, http://dx.doi.org/10.1016/j.jqsrt.2017.03.004 (2017).

[6] Green, A.A., M. Berman, P. Switzer, and M.D. Craig, "A Transformation for Ordering Multispectral Data in Terms of Image Quality with Implications for Noise Removal," IEEE Transactions on Geoscience and Remote Sensing, 26(1), 6574 (1988).

[7] Bjorgan, A., and Randeberg, L.L., "Real-Time Noise Removal for Line-Scanning Hyperspectral Devices Using a Minimum Noise Fraction-Based Approach," Sensors (Basel, Switzerland), 15(2), 3362-3378, doi:10.3390/s150203362 (2015).

[8] Phillips, R.D., L.T. Watson, C.E. Blinn and R.H. Wynne, "An adaptive noise reduction technique for improving the utility of hyperspectral data," Pecora 17, The Future of Land Imaging...Going Operational, Denver, CO, (November 18 – 20, 2008).

[9] Adler-Golden, S.M., "Signal-to-noise Enhancement," U.S. Patent Application No. 15,808,063 (November 2017).

[10] Holma, H., T. Hyvärinen, A-J. Mattila, O. Weatherbee, "Advances in hyperspectral LWIR pushbroom imagers," Proc. SPIE 8032, p. 80320X, doi:10.1117/12.884078 (2011).

[11] Achal, S., McFee, J.E., T. Ivanco and C. Anger, "A thermal infrared hyperspectral imager (TASI) for buried landmine detection," Proc. SPIE 6553, Detection and Remediation Technologies for Mines and Minelike Targets XII, 655316; doi: 10.1117/12.720453 (7 May 2007).

[12] Sundberg, R., Adler-Golden, S.M., and Conforti, P., "Long-wavelength infrared hyperspectral data mining at Cuprite, NV," Proc. SPIE 9611, Imaging Spectrometry XX, 961107 (2015).

[13] McDowell, M.L.; Kruse, F.A., "Enhanced Compositional Mapping through Integrated Full-Range Spectral Analysis," Remote Sensing, 8, 757 (2016).